

# Joint Kinematics, Kinetics and Muscle Synergy Patterns During Transitions Between Locomotion Modes

Yi-Xing Liu  and Elena M. Gutierrez-Farewik 

**Abstract**—There is an increasing demand for accurately predicting human movement intentions. To be effective, predictions must be performed as early as possible in the preceding step, though precisely how early has been studied relatively little; how and when a person's movement patterns in a transition step deviate from those in the preceding step must be clearly defined. In this study, we collected motion kinematics, kinetics and electromyography data from 9 able-bodied participants during 7 locomotion modes. Twelve types of steps between the 7 locomotion modes were studied, including 5 continuous steps (taking another step in the same locomotion mode) and 7 transitions steps (taking a step from one locomotion mode into another). For each joint degree of freedom, joint angles, angular velocities, moments, and moment rates were compared between continuous steps and transition steps, and the relative timing during the transition step at which these parameters diverged from those of a continuous step, which we refer to as transition starting times, were identified using multiple analyses of variance. Muscle synergies were also extracted for each step, and we studied in which locomotion modes these synergies were common (task-shared) and in which modes they were specific (task-specific). The transition starting times varied among different transitions and joint degrees of freedom. Most transitions started in the swing phase of the transition step. These findings can be applied to determine the critical timing at which a powered assistive device must adapt its control to enable safe and comfortable support to a user.

**Index Terms**—Biomechanics, intent recognition, and locomotion modes.

## I. INTRODUCTION

**W**EARABLE assistive devices such as exoskeletons have been extensively developed over the last several decades

Manuscript received 25 June 2022; revised 18 August 2022; accepted 15 September 2022. Date of publication 21 September 2022; date of current version 20 February 2023. This work was supported through generous support by the Promobilia Foundation (reference nr 18200) and the Swedish Research Council (reference 2018-00750 BADASS: BiomechAnics in motion Disorders and ASSistance). (Corresponding author: Yi-Xing Liu.)

Yi-Xing Liu is with the KTH MoveAbility Lab, Department of Engineering Mechanics, KTH Royal Institute of Technology, 114 28 Stockholm, Sweden (e-mail: lyixing@kth.se).

Elena M. Gutierrez-Farewik is with the KTH MoveAbility Lab, Department of Engineering Mechanics, KTH Royal Institute of Technology, Sweden, and also with the Karolinska Institute, Department of Women's and Children's Health, Sweden.

Digital Object Identifier 10.1109/TBME.2022.3208381

for both able-bodied people and people with movement disorders [1]. There is a generalized control framework for assistive devices consisting of three control levels [2]. In high-level control, user movement intention is perceived. In mid-level control, desired assistive trajectories, for instance, joint angles and joint moments, are decided while the device adjusts the state based on the perceived user intention. In low-level control, actuators are directly controlled to track the desired assistive trajectories. Accurately detecting user movement intention is thus important for assistive devices to provide precise control and achieve smooth transitions between different locomotion modes [3].

Multiple machine learning algorithms have been used to detect human movement intentions, such as linear discriminant analysis (LDA), support vector machine (SVM), k-nearest neighbours algorithm, Mahalanobis distance, and artificial neural networks (ANN) [4], [5], [6], [7]. Besides machine learning algorithms, Gaussian-based algorithms, electromyography (EMG)-driven musculoskeletal model-based approaches, and muscle synergy-inspired methods have also been used to detect movement intentions. For instance, Tanghe et al. used a Kalman filter to estimate gait phases and gait trajectories [8]. Sartori et al. used an EMG-driven musculoskeletal models to generate current movements [9]. Afzal et al. [10] and the current authors in an recent study, Liu et al. [11], used muscle synergy-inspired methods to predict movement intentions. Those methods were reported as demonstrating high accuracy in identifying either movement intentions or the current locomotion mode. However, the prediction time has seldom been measured and discussed. Authors in several studies have defined the prediction time for a transition as the time when the intention to this transition was detected accurately prior to toe-off during transitions or prior to the first heel-strike into the new locomotion mode. For instance, Huang et al. [12] presented the prediction time for identifying transitions using SVM and LDA from EMG data alone or with fused EMG and mechanical sensor data. In an recent study (Liu et al. [11]) we presented a methods that accurately predicts a person's intention to transition between locomotion modes 300-500 ms ahead of the leading limb stepping into the new mode; these prediction times were defined as the time when the classifier could detect the transition based on wearable sensor data. How these times coincide with the actual and noticeable changes in movement kinematics and kinetics, i.e. the time

that is critical for a controller to adapt to a new locomotion mode, is not entirely known. In other words, as the critical prediction time has not been identified consistently, it is difficult to evaluate and compare the efficacy of different prediction methods.

For a user of a controlled assistive device, accurate and timely detection of movement intention is essential to reduce the risks of falling and tripping [13]. To this end, Zhang et al. [13], conducted experiments in completing four transitions, namely from level ground walking to ramp ascent and descent, and vice versa, with seven participants wearing powered knee prostheses. They switched control modes in the powered knee prostheses at different times during the four transitions, and observed whether participants could complete the transitions without stopping. While they confirmed their earlier defined critical timings [12], switching control mode after the defined critical timing did not always influence users' walking balance.

Several other studies have instead defined the starting times of step-to-step transitions based on biomechanical parameters. Grimmer et al. [14] identified the starting and ending times of transitions between level ground walking and stair ascent and descent based on joint kinematics and kinetics. Other studies have identified biomechanical parameters that may indicate when elderly persons are at risk for their first fall based on comparing participants' biomechanical parameters between the young and the elderly group [15], [16]. While this approach may be a more effective strategy for control of assistive devices, such studies are few in number and limited in studied transitions. For reliable and genuinely useful wearable assistive devices in daily life, investigating more transitions, for instance, from level ground walking to stepping over an obstacle and to standing still, are needed to achieve safe and comfortable control in a spectrum of daily scenarios.

Yet another approach has been to study mechanics, energetics [17], and muscle synergy patterns during transitions [18], [19], [20]. In the context that muscle synergies are defined as a fixed relative action level of different muscles, muscle synergy has been used in movement intention detection, in muscle activation estimation, in joint moment prediction, and in exoskeleton control. For instance, Rasool et al. [21] used task-specific muscle synergies to classify different upper limb activities, and Garate et al. [22] used the concept of muscle synergy in a unilateral lower limb exoskeleton control. Most studies report the use of the non-negative matrix factorization algorithm (NMF) to extract muscle synergies [23], [24] from filtered EMG signals. Several studies report extracting muscle synergies from principle activation by pre-processing EMG signals using a hierarchical clustering algorithm [25] and investigating how muscle synergies were influenced by pre-processing methods [26]. Muscle synergies have been observed to be common to different locomotion modes or "task-shared," for instance, between walking and ramp walking [27], while others have been observed as specific for different locomotion modes, or "task-specific," for instance between walking and running [19]. Identifying which muscle synergies are task-shared and which are task-specific during not only different locomotion modes but also during transitions can

be informative for methods that use muscle synergies to detect movement intention predictions or to predict joint moments.

In a context of effective and timely detection of a person's movement intentions, the overall objective of this study was to provide useful and practical information about a person's kinematics, kinetics and muscle activity patterns during transitions between locomotion modes. The first specific aim was to define the transition starting times of 7 transition steps in four joint degrees of freedoms (DOFs) based on measured joint kinematics and kinetics. The second specific aim was to study whether there are periods in transition steps that are unique, i.e. in which the kinematics and kinetics diverge from continuous steps in the mode before and in the mode after the transition. The third specific aim was to identify muscle synergy patterns during these transitions, and to determine whether they were common among different transitions or whether they were specific to certain transitions.

## II. METHOD

### A. Participants

Nine subjects without any musculoskeletal disorders or recent lower-extremity injuries (6F/3 M, height:  $171.6 \pm 9.8$  cm, mass:  $64.4 \pm 11.5$  kg, age:  $29.4 \pm 2.4$  years) took part in the study. The experiments were approved by the Swedish Ethical Review Authority (Dnr. 2020-02311). All subjects provided written consent. Participation was voluntary and could be terminated at any time.

### B. Experimental Protocol and Data Collection

Experiments were conducted in the KTH MoveAbility Lab, equipped with a 10-camera motion capture system (Vicon V16), 4 floor-mounted force plates (AMTI, 60 cm  $\times$  40 cm), 1 portable force plate (AMTI), and wireless EMG (Myon aktos). Surface EMG data were recorded on 12 muscles on the right limb – gluteus maximus (GMa), gluteus medius (GMe), rectus femoris (RF), vastus medialis (VM), vastus lateralis (VL), biceps femoris (BF), semitendinosus (ST), tibialis anterior (TA), soleus (Sol), medial and lateral gastrocnemius (MGas and LGas), and peroneus longus (PL). EMG electrodes were placed according to SENIAM recommendations [28]. Forty-three motion capture markers were placed on each subject according to the CGM 2.3 full-body model [29]. EMG and force plate data were sampled at 2000 Hz and marker data were sampled at 100 Hz.

A tailored ramp module ( $8^\circ$ ) with an embedded portable force plate (50 cm  $\times$  25 cm) and a tailored 3-stair module with 18 cm rise and 28 cm run, capable of measuring ground reaction forces on each of the 3 steps, were used in experiments (Fig. 1). Each participant performed 7 locomotion modes, namely, level ground walking (W), ramp ascent (RA), ramp descent (RD), stair ascent (SA), stair descent (SD), stepping over an obstacle (O) with 20 cm high, and standing still (ST), and the transitions among them. We were able to measure ground reaction forces (GRFs) during all transitions except 2:  $W \rightarrow RD$  and  $W \rightarrow SD$ ; our tailored ramp module lacked a force plate on

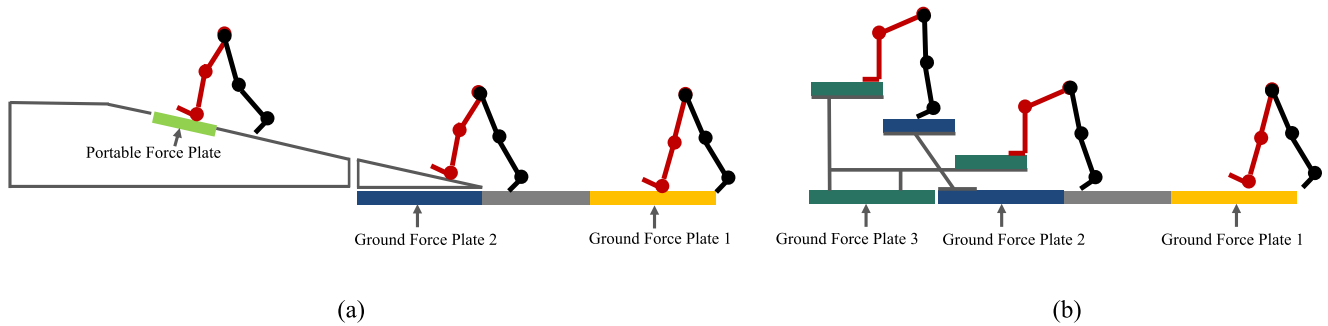


Fig. 1. Illustrations of the tailored ramp module used in experiments, including placement of force plates. Continuous and transition steps were performed by the right leg, shown in red. (a) Ground and portable force plates were used to measure GRF to and from ramp walking; (b) The stairs module was constructed so that GRF could be collected on the ground and on all 3 stairs.

TABLE I  
THE 7 LOCOMOTION MODES AND THE 12 STEPS BETWEEN THEM, INCLUDING 5 CONTINUOUS STEPS AND 7 TRANSITION STEPS

Mode	Level Ground Walking (W)	Ramp Ascent (RA)	Ramp Descent (RD)	Stair Ascent (SA)	Stair Descent (SD)	Stepping Over an Obstacle (O)	Standing Still (ST)
Continuous step in same mode	W→W	RA→RA	RD→RD	SA→SA	SD→SD	×	×
Transitions from one mode to another	W→RA, W→SA, W→O, W→ST	RA→W	RD→W	×	SD→W	×	×

the raised platform. Thus, we studied 12 steps among those 7 locomotion modes (Table I), including 5 continuous steps, i.e. another step from one locomotion mode into the same mode, and 7 transitions, i.e. a step from one locomotion mode into another. To obtain natural gait patterns, we did not ask participants to hit every force plate during each trial. Ground reaction force of each continuous step and transition step was collected by adjusting the starting position for each participant in order to obtain data from at least one force plate per trial. This procedure was repeated until data from at least 15 trials were collected. The order of stair and ramp walking was randomized. During data collection, all participants were also encouraged to walk at a self-selected, comfortable speed and to try to maintain this speed as closely as possible. All continuous and transition steps were performed by the right leg.

### C. Data Post-Processing

All EMG signals were band-pass filtered (20-400 Hz, Butterworth 4th order), rectified, and low-pass filtered (4 Hz, Butterworth 4th order). All negative values after the low-pass filter were replaced by zero. For each participant, each EMG signal was normalized to its maximum during the whole session.

The phases of gait are described according to reference [30]. Stance phase was defined as the duration between foot-strike and toe-off, and swing phase was defined as the duration between the toe-off and foot-strike, where foot-strike could involve initial contact of the heel, toe, or forefoot. Foot-strike and toe-off were detected by the force plates, compliant with

manual checks. Strides were defined as a stance phase and subsequent swing phase, analyzed for the right leg. Within a stride, joint angles ( $A$ ) and moments ( $M$ ) on the right limb were computed for 4 joint DOFs: hip ab/adduction (Hip\_AB), hip flexion/extension (Hip\_FE), knee flexion/extension (Knee\_FE), and ankle dorsi/plantarflexion (Ankle\_DP) through inverse kinematics and inverse dynamics (Vicon Nexus with CGM 2.3 fitting [31]). Joint moments were normalized into range of  $[-1, 1]$  based on maximum and minimum values within each stride. For each joint angle and moment, angular velocity ( $V$ ) and moment rate ( $R$ ) were computed through discrete differentiation. For each participant and each transition,  $A$ ,  $M$ ,  $V$ , and  $R$  were computed for at least 10 strides, normalized to percent stance phase and percent swing phase, and then averaged among trials. A trailing moving average filter with a sliding window of 10% of a stride cycle and 1% increment was used to filter  $A$ ,  $M$ ,  $V$ , and  $R$ , to minimize discontinuities due to slightly different toe-off timing (Fig. 2(a) and (b)).

### D. Identifying the Starting Times of Transitions

For each of the 7 transitions, each of the 4 joint DOFs and at each time step, the average time series variables  $A$ ,  $M$ ,  $V$ , and  $R$  at each time step were compared to those from the continuous steps in the same mode using multiple analysis of variance (MANOVA) and a significance level of 0.05. Before running MANOVA, the normality of multivariate data distribution was evaluated by a Henze-Zirkler test. For all multivariate tests,  $p > 0.05$  indicates that the null hypothesis of normal distributed

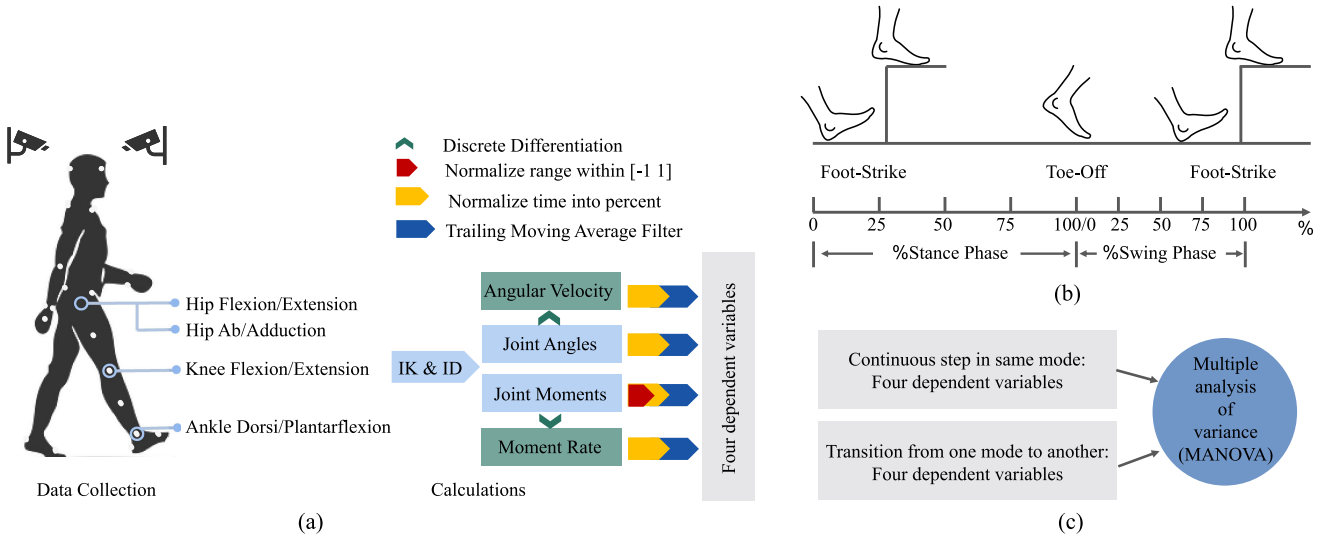


Fig. 2. Process of conducting a multiple analysis of variance (MANOVA). (a) Kinematics and kinetics data acquisition and analysis for each participant and each transition. IK & ID: inverse kinematics and inverse dynamics; (b) Normalization of kinematics and kinetics parameters as percent of stance phase and of swing phase; (c) The time that the kinematics and kinetics parameters in the transition diverged from those in continuous steps was determined with MANOVA analyses.

could not be rejected. Transition starting time was defined as the time when the 4 time-series variables in the transitions significantly diverged from those in the continuous steps in that locomotion mode, and were defined separately for each joint ROM [14], [32] (Fig. 2(c)). For the 4 transitions from walking, divergence of the 4 variables was studied during both stance and swing phases. For the transitions from ramp ascent, ramp descent and stair descent, divergence during only the swing phase was studied; as the relatively short ramp and stair module limited the amount of stance phase data we could collect in continuous steps.

For each transition step, we also identified the starting times based on inter-joint analysis in the sagittal plane, including Hip\_FE, Knee\_FE, and Ankle\_DP. MANOVA analyses were run with 12 dependent variables comprised of the four variables from each joint DOF.

### E. Identifying Unique Transition Duration

For transitions of  $W \rightarrow RA$  and  $W \rightarrow SA$ , comparisons of the 4 time-series variables were also made between  $W \rightarrow RA$  and  $RA \rightarrow RA$  and between  $W \rightarrow SA$  and  $SA \rightarrow SA$  with MANOVAs to study the unique transition duration during these two transitions. Unique transition duration in a transition was defined as the duration when the four dependent variables in a transition diverged both from those in the continuous steps of the mode before and of the mode after the transition.

### F. Identifying Muscle Synergies

Muscle synergies were extracted using the non-negative matrix factorizing algorithm (NMF),

$$W, H = \text{NMF}(E), \quad \min_{W, H} |W \times H - E| \quad (1)$$

where  $E$  is the data set of all 12 filtered EMGs.  $W$  has  $12 \times n_{ms}$  dimensions, and  $H$  has  $n_{ms} \times n_{time}$  dimensions, where  $n_{ms}$  is the number of muscle synergies, and  $n_{time}$  is the number of time frames used to extract muscle synergies.

The variance accounted for ( $v_{af}$ ) describes the explained variance between an original data set  $y$  and an estimated data set  $\hat{y}$ , i.e. between the set of 12 EMG signals  $E$  and the reconstructed  $\tilde{E}$ . The  $v_{af}$  in percent is defined as:

$$\tilde{E}_i \cong \sum W_{ij} \times H_j, \quad i = 1, 2, 3, \dots, 12, j = 1, 2, 3, \dots, n_{ms} \quad (2)$$

$$v_{af} = \left(1 - \frac{\text{Variance}(y - \hat{y})}{\text{Variance}(y)}\right) \times 100\% \quad (3)$$

The number of muscle synergies was decided by the  $v_{af}$  as follows:  $n_{ms}$  was determined when the averaged  $v_{af}$  among subjects was above 90% and did not increase more than 5% when the number of muscle synergies increased, similar to previous studies [33], [34]. We added a further local criterion that muscle synergies also accounted for greater than 80% VAF in each muscle and each perturbation direction [19], [35]

The uncentered correlation coefficient  $r_{\text{uncentered}}$  was used to measure the similarity between a pair of muscle synergies [33].

$$r_{\text{uncentered}} = \frac{\sum_{i=1}^N (x_i \times y_i)}{\sqrt{\sum_{i=1}^N x_i^2 \times \sum_{i=1}^N y_i^2}} \quad (4)$$

in which  $x$  and  $y$  were muscle synergy weight vectors in continuous and transition steps and  $N$  was the number of EMG in each muscle synergy weight vector. For each transition, we randomly selected the order of muscle synergies in one subject as the reference, and then reordered the muscle synergies in other subjects as the same order based on the similarities between each pair of muscle synergy weights. This process was conducted



TABLE II

THE AVERAGE (MEAN  $\pm$  STD) STRIDE TIME (MS) FOR 12 STEPS ACROSS PARTICIPANTS, INCLUDING 4 CONTINUOUS STEPS AND 8 TRANSITION STEPS

Step	Time (ms)
Continuous and transition steps from Walking (W)	
W $\rightarrow$ W	1073 $\pm$ 66
W $\rightarrow$ RA (Ramp Ascent)	1056 $\pm$ 46
W $\rightarrow$ ST (Standing Still)	1079 $\pm$ 59
W $\rightarrow$ O (Stepping over obstacle)	1244 $\pm$ 100
W $\rightarrow$ SA (Stairs Ascent)	1094 $\pm$ 46
Continuous and transition steps from Ramp Ascent	
RA $\rightarrow$ RA	1091 $\pm$ 148
RA $\rightarrow$ W	1243 $\pm$ 86
Continuous and transition steps from Ramp Descent	
RD $\rightarrow$ RD	1063 $\pm$ 76
RD $\rightarrow$ W	1005 $\pm$ 51
Continuous and transition steps from Stairs Ascent	
SA $\rightarrow$ SA	1236 $\pm$ 106
SA $\rightarrow$ W	1349 $\pm$ 99
Continuous and transition steps from Stairs Descent	
SD $\rightarrow$ SD	1346 $\pm$ 158
SD $\rightarrow$ W	1090 $\pm$ 83

by using a hierarchical clustering method with the metric of  $r_{\text{uncentered}}$ . Similarly, for each subject, we used the hierarchical clustering method to find common muscle synergies among different transitions, referred to as task-shared synergies. A pair of synergies was considered significantly similar if  $r_{\text{uncentered}} > 0.7$ , and marginally similar if  $r_{\text{uncentered}} > 0.45$  [36]. Pairs of muscle synergies that were not found to be task-shared were considered as task-specific.

To investigate the similarity of muscle synergy weights across steps, we calculated the  $v_{\text{af}}$  of using the muscle synergy weights of the continuous step W  $\rightarrow$  W to reconstruct the muscle excitation  $\tilde{E}$  of the four transition steps. [35], [37].

### III. RESULTS

#### A. The Transitions Originated From W

The average stride time across participants were 1000-1350 ms for all 12 steps (Table II). Transition starting times were observed in all transitions from level ground walking and in all four joint DOFs, starting times and even durations of divergence varied (Fig. 3). Starting times and unique durations are described for each transition below.

Starting time of the W  $\rightarrow$  RA transition were in early swing in Ankle\_DP and in mid- to late swing in the other joint DOFs. Durations unique to this transition were found in Hip\_FE and

TABLE III

THE EXPLAINED VARIANCE FOR ( $v_{\text{af}}$ ) ACROSS PARTICIPANTS OF USING THE MUSCLE SYNERGY WEIGHTS ( $n_{\text{MS}} = 5$ ) OF THE STEP FROM WALKING TO WALKING (W) TO RECONSTRUCT THE MUSCLE EXCITATION OF THE FOUR TRANSITION STEPS FROM WALKING

Transition Step	$v_{\text{af}}$ (mean $\pm$ std%)
W $\rightarrow$ RA (Ramp Ascent)	42 $\pm$ 16
W $\rightarrow$ ST (Standing Still)	39 $\pm$ 30
W $\rightarrow$ O (Stepping over obstacle)	23 $\pm$ 15
W $\rightarrow$ SA (Stairs Ascent)	29 $\pm$ 27

Knee\_FE both briefly during early to mid-stance and longer during mid- to late swing. Relatively short unique durations were observed in Hip\_AB and Ankle\_DP in early and mid-swing (Fig. 4). Starting time of the W  $\rightarrow$  RA transition using inter-joints analysis was in late swing (Fig. 5).

Starting time of the W  $\rightarrow$  ST transition occurred in swing in all joint DOFs; in early swing in Ankle\_DP and in late swing in the other three joint DOFs. When using inter-joints analysis, no significant difference was found in the 12 variables of the W  $\rightarrow$  ST transition to these in the W  $\rightarrow$  W step.

Starting times of the W  $\rightarrow$  O transition occurred earliest; transition started in mid- to late stance in Hip\_FE and Ankle\_DP, and in early to mid-swing in Hip\_AB and Knee\_FE, similar to the starting time identified by inter-joints analysis.

Starting times of the W  $\rightarrow$  SA transition occurred also relatively early in most joint DOFs. Starting time was in early swing in Hip\_FE and Knee\_FE, with a very short but not lasting duration of divergence in early stance in Hip\_FE. Starting time in Hip\_AB was the latest (late swing), while a brief divergence in Ankle\_DP was observed in late stance. Relatively long durations unique to this transition were observed in swing phase in Hip\_FE, Knee\_FE and Ankle\_DP, and shorter durations were observed in early stance in Hip\_FE and late stance in Ankle\_DP. No durations of unique transition were observed in Hip\_AB. Starting time of the W  $\rightarrow$  SA transition using inter-joints analysis was observed in swing phase.

For the 5 continuous and transition steps from W, an average  $v_{\text{af}}$  above 90% (Fig. 6) and local  $v_{\text{af}}$  above 80% (Fig. 7) were achieved when five muscle synergies were extracted. The numbers and groups of the task-shared and task-specific muscle synergies were different among participants and transitions (Fig. 8). Generally, there were 3-4 task-shared muscle synergy patterns and 1-2 task-specific muscle synergy pattern between each transition and W  $\rightarrow$  W for each participant (Fig. 9). The  $v_{\text{af}}$  lower than 50% were achieved for the four transition steps from walking when using the extracted muscle synergy weights ( $n_{\text{ms}} = 5$ ) of the continuous step W  $\rightarrow$  W to reconstruct the muscle excitation (Table III).

#### B. The Transitions Originated From RA, RD, and SD

Starting times of the RA  $\rightarrow$  W transition occurred in early swing in Hip\_FE and Knee\_FE and in mid- to late swing in

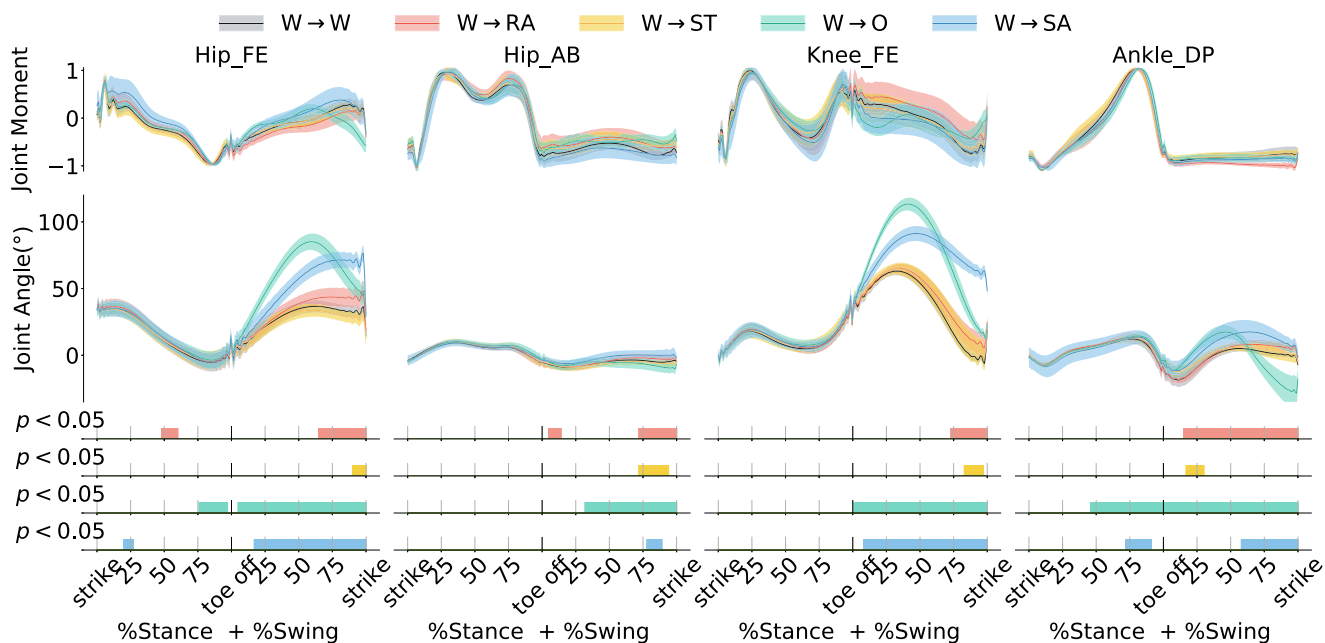


Fig. 3. Joint angles and moments during continuous steps in level ground walking ( $W \rightarrow W$ ) and from 4 transitions from level ground walking to ramp ascent ( $W \rightarrow RA$ ), to standing still ( $W \rightarrow ST$ ), to stepping over an obstacle ( $W \rightarrow O$ ), and to stair ascent ( $W \rightarrow SA$ ). Joint moments for four joint DOFs – hip flexion/extension (FE), hip ab/adduction (AB), knee flexion/extension (FE), and ankle dorsi/plantarflexion (DP) – were normalized based on the maximum and minimum moments from each trial. For the four transitions, statistical difference ( $p < 0.05$ ) to  $W \rightarrow W$  according to MANOVA analyses are indicated as time-series data.

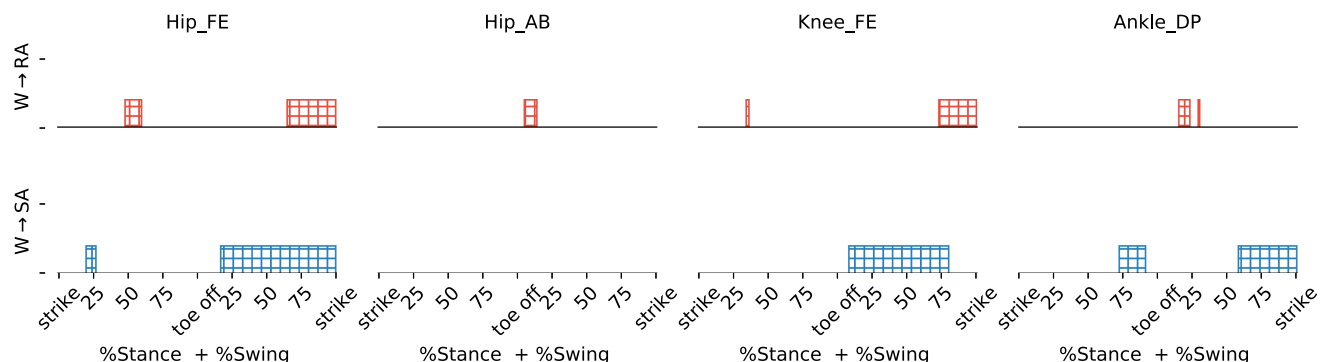


Fig. 4. Durations of transitions from level ground walking to ramp ascent ( $W \rightarrow RA$ ) and to stairs ascent ( $W \rightarrow SA$ ) when the transition was unique, i.e. when the kinematic and kinetics parameters diverged from both  $W \rightarrow W$  and from  $RA \rightarrow RA$  (top) or  $SA \rightarrow SA$  (bottom), according to analyses with MANOVAs, are indicated, in the four joint degrees of freedom hip flexion/extension (FE), hip ab/adduction (AB), knee flexion/extension (FE), and ankle dorsi/plantarflexion (DP).

Hip\_AB and Ankle\_DP (Fig. 10). Starting time of the  $RA \rightarrow RA$  transition using inter-joints analysis was in early swing (Fig. 11).

Starting times of the  $RD \rightarrow W$  transition occurred right at toe-off in Hip\_FE, Knee\_FE and Ankle\_DP, but in late stance in Hip\_AB. When using inter-joints analysis, no significant difference was found in which the 12 variables of the  $RD \rightarrow W$  transition to these in the  $RD \rightarrow RD$  step.

Starting times of the  $SD \rightarrow W$  transition occurred right at toe-off in Hip\_FE and Ankle\_DP and in early to mid-swing in Hip\_AB and Knee\_FE. When using inter-joints analysis, no significant difference was found in the 12 variables of the  $SD \rightarrow W$  transition to these in the  $SD \rightarrow SD$  step.

#### IV. DISCUSSION

The main contribution of this study is the demonstrated times at which a person's movement biomechanics, specifically joint kinematics and kinetics, distinguish themselves in a transition step as compared to continuous steps. The other main contribution was the identification of which muscle synergies are common among different transitions.

Starting times were varied among transitions and joint DOFs; some occurred as early as mid-stance in the transition step, while most occurred during the swing phase. These are important to consider along with prediction times of algorithms aimed to detect a person's movement intentions. In order for an algorithm

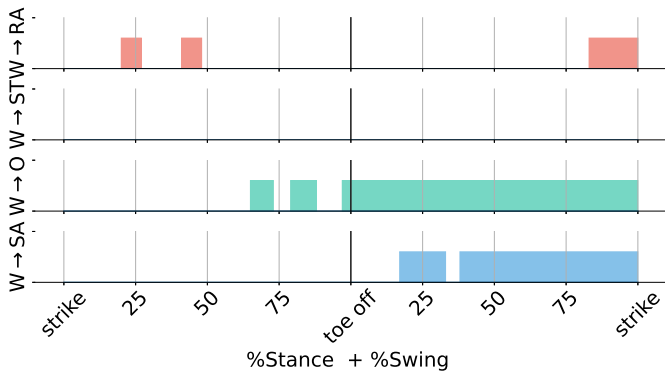


Fig. 5. For the transition steps from level ground walking (W), statistical difference ( $p < 0.05$ ) to  $W \rightarrow W$  from inter-joints analyses according to MANOVA analyses are indicated as time-series data. From top to bottom,  $W \rightarrow RA$  (Ramp Ascent),  $W \rightarrow ST$  (Standing still),  $W \rightarrow O$  (Stepping over an obstacle), and  $W \rightarrow SA$ (stairs Ascent) are shown as one transition per row respectively.

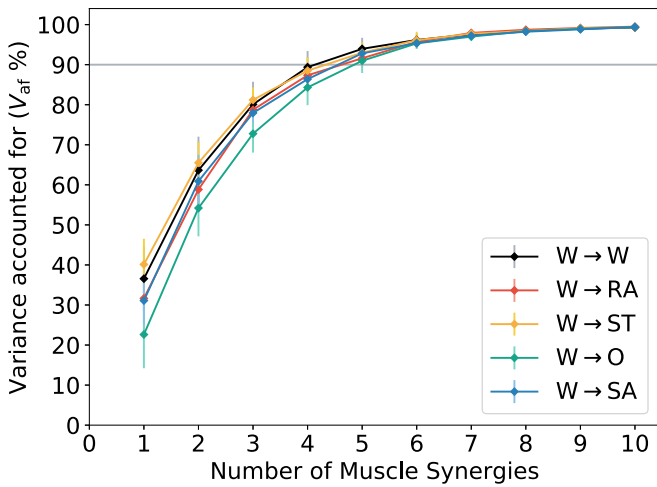


Fig. 6. For the continuous and transition steps from level ground walking (W), the variance accounted for  $v_{af}$  when extracting 1-10 numbers of muscle synergies. RA: ramp ascent; ST: standing still; O: stepping over an obstacle; SA: stairs ascent.

that detects a person’s intention to transition to be effective and useful in, for example, the controller of an assistive device, this prediction must have occurred before the transition actually begins, in order for the controller to adapt to a new locomotion mode. In this way, the starting times identified in this study can be seen as critical timing for detection of movement intention. As a specific example, from a level ground walking mode, a powered assistive device must accurately detect a person’s intention to step over an obstacle quite early in the preceding stance phase, but need only detect the intention to stand still rather late in the preceding swing phase.

The starting times for all transitions varied among joint DOFs, which suggests that control should be specific for different joints and motions. Several studies of detecting movement intentions report prediction time of 300-500 ms ahead of the leading limb stepping into the new locomotion mode [11], of 130-260 ms prior to gait initiation [38], and around toe-off events [10], [12].

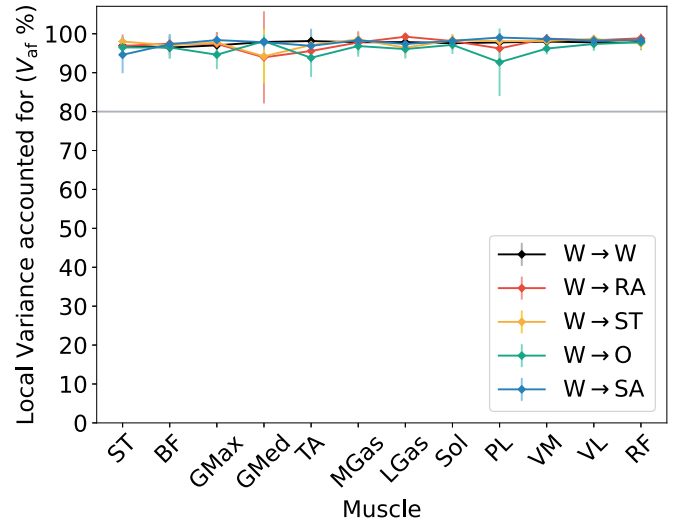


Fig. 7. For the continuous and transition steps from level ground walking (W), the local variance accounted for  $v_{af}$  for each muscle when extracting five muscle synergies. RA: ramp ascent; ST: standing still; O: stepping over an obstacle; SA: stairs ascent; ST: semitendiosus, BF: biceps femoris, GMax: gluteus maximus, GMed: gluteus medius, TA: tibialis anterior, MGas: medial gastrocnemius, LGas: lateral gastrocnemius, Sol: soleus, PL: peroneus longus, VM: vastus medialis, VL: vastus lateralis; RF: rectus femoris.

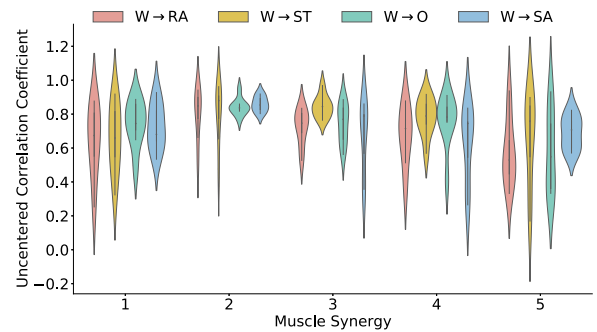
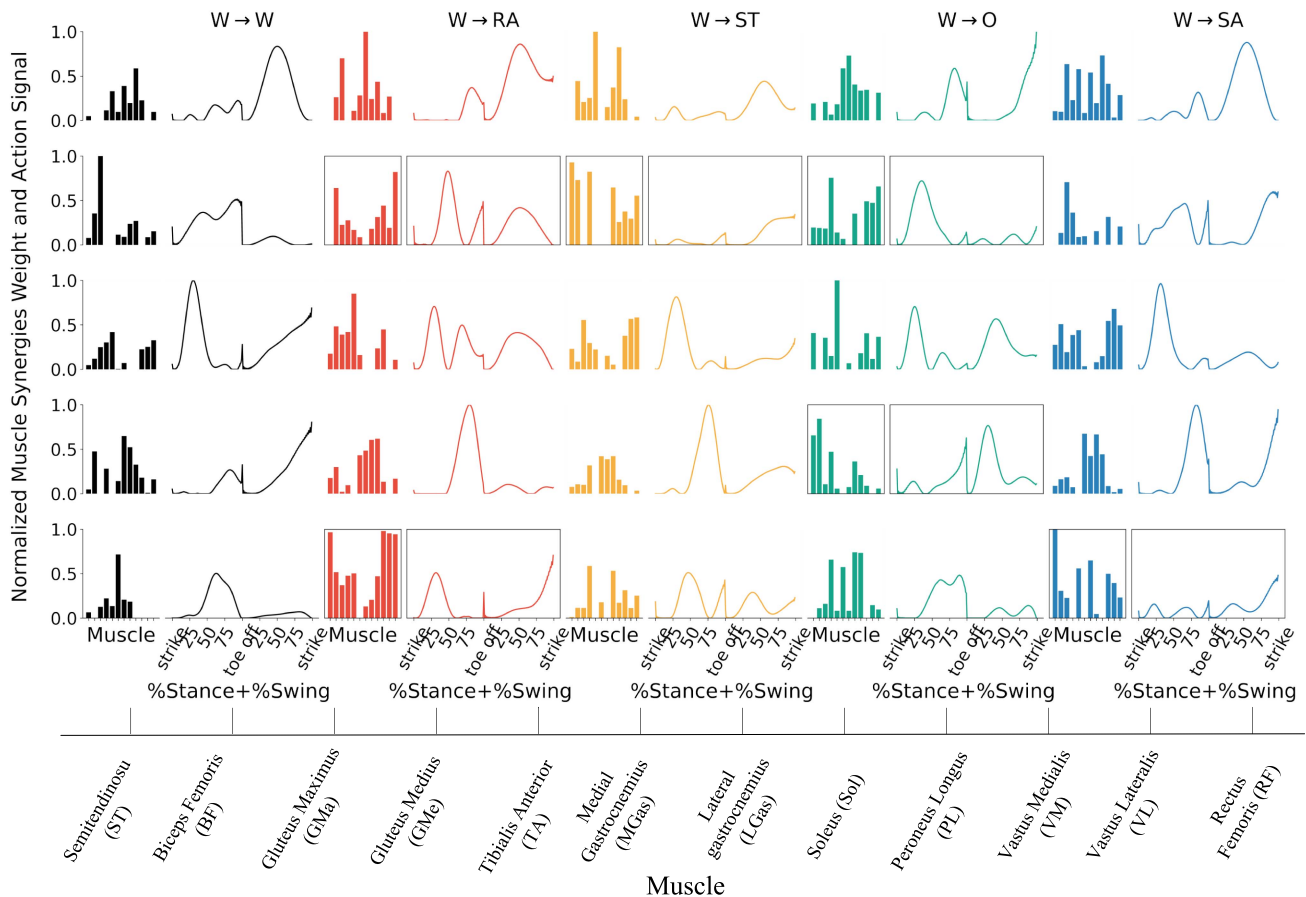


Fig. 8. For the four transitions from level ground walking, the uncentered correlation coefficients ( $r_{ucc}$ ) between each transition and the continuous step for each muscle synergy are presented. W: level ground walking; RA: ramp ascent; ST: standing still; O: stepping over an obstacle; SA: stairs ascent.

The identified starting times in our study suggested that these prediction times may be adequate for exoskeleton control in most cases. Interestingly, inter-joint analyses did not always improve identification of transition starting times. No transition starting time was found in the transition steps of  $W \rightarrow ST$ ,  $RD \rightarrow W$ , and  $SD \rightarrow W$ . This finding implies that the inter-joints analyses could not always be indicative enough to determine the critical timing for assistive devices to switch assistive modes that allow safe and seamless task transitions.

The observations that some durations were unique to  $W \rightarrow RA$  and  $W \rightarrow SA$  in both stance and swing phases indicate that, to transit smoothly, the dedicated and specific assistive trajectories which are different from the continuous steps may be needed for these transition phases.



**Fig. 9.** Example results from one participant showing the normalized muscle synergy weights and action signals for the four transition steps from level ground walking and the continuous step ( $W \rightarrow W$ ). For each step, muscle synergy action signals were averaged among several strides, normalized to the maximum action signal values, normalized along time into 100% stance phase + 100% swing phase, shown as one muscle synergy per row. Muscle synergy weights of each step were normalized to the maximum weight values were shown as bar plots. Muscle synergy action signals of each step were shown as curve plots, respectively,  $W \rightarrow W$  in black,  $W \rightarrow RA$  (ramp ascent) in red,  $W \rightarrow ST$  (standing still) in yellow,  $W \rightarrow O$  (stepping over an obstacle) in green, and  $W \rightarrow SA$  (stair ascent) in blue. For each pair of transitions, task-specific muscle synergies are indicated with boxes.

Our findings that the starting time of  $W \rightarrow SA$  in Hip\_FE and Knee\_FE were in the early swing phase agrees with findings by Grimmer et al. [14]. Similarly, the findings that unique transition durations existed during the  $W \rightarrow SA$  transition and that starting times were earlier in the knee and ankle joints than at the hip also agrees with the findings in [14]. That this transition started early in Ankle\_DP may be related to the demand at the angles to lift the body center of mass upward. The ankle joint muscles contribute more to propulsion and support than do muscles at the knee and hip [39]. We may attribute similar findings about starting times during the  $W \rightarrow O$ , in which the transition began earlier at the ankle than at the knee or hip. In contrast, in stair descent and the transitions from it, foot placement of the leading limb might be more critical than propulsion; transition started early in the hip and knee joints in the  $SD \rightarrow W$ .

That short durations of diverging kinematics and kinetics from  $W \rightarrow W$  were found during stance in  $W \rightarrow SA$  are difficult to interpret. It may be that the transition actually begins very early, but it could also be attributable to inter-subject variability in trunk [40] or other joint postures or to the variation in timing of defined gait events. Similar findings in  $W \rightarrow RA$  may be

attributed to the same reason. It is also possible that the early but not sustained transition in  $W \rightarrow RA$  does reflect kinematic changes in anticipation of the next step. That the earliest sustained transition was observed in the ankle may reflect early pre-positioning of the foot for the subsequent step on an inclined surface.

Our findings five extracted muscle synergies achieved high  $v_{af}$  and that muscle synergies tended to be subject-specific agree with numerous muscle synergy studies [19], [36], [41]. The finding that there was at least one task-specific muscle synergy for most transitions agrees with those from muscle synergy-inspired methods for predicting movement intentions [10] and controlling exoskeletons to achieve discrimination tasks [21]. The presence of task-shared muscle synergies suggests the generalizability of muscle synergy-inspired methods among different movements, for instance, using muscle synergies to predict EMG signals [42] and lower limb joint moments.

One limitation in our study was that the lab size, the length of the tailored ramp module and the number of steps in the stairs module were not enough for participants to take multiple continuous steps in ramp and stair modes. As such, we could



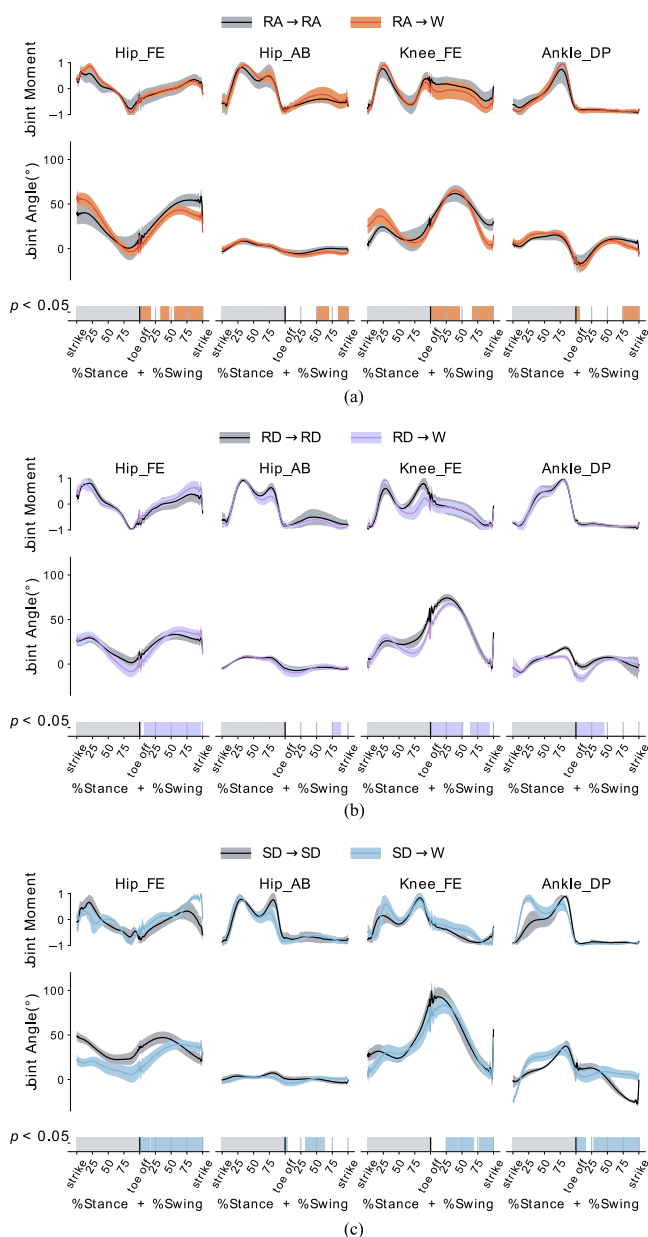


**Fig. 10.** Joint angles and moments during continuous and transitions from (a) ramp ascent (RA), (b) ramp descent (RD) and (c) stairs descent (SD) to level ground walking (W). Joint moment for four joint DOFs – hip flexion/extension (FE), hip ab/adduction (AB), knee flexion/extension (FE), and ankle dorsi/plantarflexion (DP) – were normalized based on the maximum and minimum moments from each trial. For each transition, statistical difference ( $p < 0.05$ ) to the continuous step according to MANOVA analyses are indicated as time-series data. Note that only the swing phase was analyzed and starting times could thus occur from toe-off at the earliest.

not reliably analyze whether transitions from ramp and stair walking diverged from continuous ramp and stair walking in the stance phase; starting times of these transitions were only studied during the preceding swing phase. Our study only included able-bodied participants; our findings are thus not directly generalizable to any patient population. Studies conducted in a similar manner but with participants with motor disability should be performed. We did not specifically compute the center

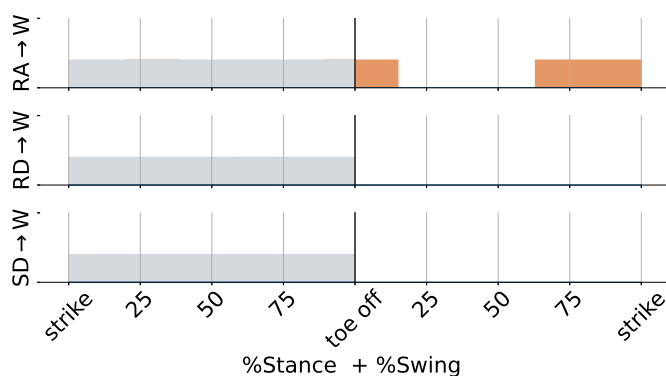


**Fig. 11.** For the transition steps from ramp ascent (RA), ramp descent (RD), and stairs descent (SD) to level ground walking (W), statistical difference ( $p < 0.05$ ) to the continuous steps from inter-joints analyses according to MANOVA analyses are indicated as time-series data. From top to bottom, RA  $\rightarrow$  W, RD  $\rightarrow$  W, and SA  $\rightarrow$  W are shown as one transition per row respectively. Note that only the swing phase was analyzed and starting times could thus occur from toe-off at the earliest.

of mass velocity in our study, which may be interesting from the perspective of balance [13]. It should also be noted that, in studying muscle synergies, we did not study whether there was any effect of gender in task-specific or task-shared synergy patterns [18], owing to the limited number of participants.

## V. CONCLUSION

In this study, we defined the starting times for 7 transitions in 4 joint degrees of freedom based on measured joint kinematics and kinetics. Most transitions began early in the swing phase prior to the transition, but some began as early as mid- to late stance phase. Five muscle synergies were extracted for 5 transitions. While several muscle synergies were common among different transitions, at least one task-specific muscle synergy was found. We believe that this study provides useful information for the effectiveness of the methods that detect movement intentions, including critical timings for accurate prediction.

## REFERENCES

- [1] A. M. Dollar and H. Herr, "Lower extremity exoskeletons and active orthoses: Challenges and state-of-the-art," *IEEE Trans. Robot.*, vol. 24, no. 1, pp. 144–158, Feb. 2008.
- [2] M. R. Tucker et al., "Control strategies for active lower extremity prosthetics and orthotics: A review," *J. Neuroeng. Rehabilitation*, vol. 12, no. 1, pp. 1–30, 2015.
- [3] T. Lenzi et al., "Intention-based EMG control for powered exoskeletons," *IEEE Trans. Biomed. Eng.*, vol. 59, no. 8, pp. 2180–2190, Aug. 2012.
- [4] J. A. Spanias et al., "Detection of and compensation for EMG disturbances for powered lower limb prosthesis control," *IEEE Trans. Neural Syst. Rehabil. Eng.*, vol. 24, no. 2, pp. 226–234, Feb. 2016.
- [5] O. Bai et al., "Prediction of human voluntary movement before it occurs," *Clin. Neurophysiol.*, vol. 122, no. 2, pp. 364–372, 2011.
- [6] A. Young et al., "Analysis of using EMG and mechanical sensors to enhance intent recognition in powered lower limb prostheses," *J. Neural Eng.*, vol. 11, no. 5, 2014, Art. no. 056021.
- [7] H. Huang, T. A. Kuiken, and R. D. Lipschutz, "A strategy for identifying locomotion modes using surface electromyography," *IEEE Trans. Biomed. Eng.*, vol. 56, no. 1, pp. 65–73, Jan. 2009.
- [8] K. Tanghe et al., "Gait trajectory and event prediction from state estimation for exoskeletons during gait," *IEEE Trans. Neural Syst. Rehabil. Eng.*, vol. 28, no. 1, pp. 211–220, Jan. 2020.

- [9] M. Sartori et al., "Modeling the human knee for assistive technologies," *IEEE Trans. Biomed. Eng.*, vol. 59, no. 9, pp. 2642–2649, Sep. 2012.
- [10] T. Afzal et al., "A method for locomotion mode identification using muscle synergies," *IEEE Trans. Neural Syst. Rehabil. Eng.*, vol. 25, no. 6, pp. 608–617, Jun. 2017.
- [11] Y.-X. Liu et al., "A muscle synergy-inspired method of detecting human movement intentions based on wearable sensor fusion," *IEEE Trans. Neural Syst. Rehabil. Eng.*, vol. 29, pp. 1089–1098, 2021.
- [12] H. Huang et al., "Continuous locomotion-mode identification for prosthetic legs based on neuromuscular–mechanical fusion," *IEEE Trans. Biomed. Eng.*, vol. 58, no. 10, pp. 2867–2875, Oct. 2011.
- [13] F. Zhang et al., "Investigation of timing to switch control mode in powered knee prostheses during task transitions," *PLoS One*, vol. 10, no. 7, 2015, Art. no. e0133965.
- [14] M. Grimmer et al., "Lower limb joint biomechanics-based identification of gait transitions in between level walking and stair ambulation," *PLoS One*, vol. 15, no. 9, 2020, Art. no. e0239148.
- [15] G. M. Meurisse et al., "The step-to-step transition mode: A potential indicator of first-fall risk in elderly adults ?," *PLoS One*, vol. 14, no. 8, 2019, Art. no. e0220791.
- [16] N. König et al., "Identification of functional parameters for the classification of older female fallers and prediction of 'first-time' fallers," *J. Roy. Soc. Interface*, vol. 11, no. 97, 2014, Art. no. 20140353.
- [17] C. H. Soo and J. M. Donelan, "Mechanics and energetics of step-to-step transitions isolated from human walking," *J. Exp. Biol.*, vol. 213, no. 24, pp. 4265–4271, 2010.
- [18] M. M. Nazifi et al., "Shared and task-specific muscle synergies during normal walking and slipping," *Front. Hum. Neurosci.*, vol. 11, 2017, Art. no. 40.
- [19] S. Hagio et al., "Identification of muscle synergies associated with gait transition in humans," *Front. Hum. Neurosci.*, vol. 9, 2015, Art. no. 48.
- [20] Y. Choi et al., "Muscle synergies for turning during human walking," *J. Motor Behav.*, vol. 51, no. 1, pp. 1–9, 2019.
- [21] G. Rasool et al., "Real-time task discrimination for myoelectric control employing task-specific muscle synergies," *IEEE Trans. Neural Syst. Rehabil. Eng.*, vol. 24, no. 1, pp. 98–108, Jan. 2016.
- [22] V. R. Garate et al., "Experimental validation of motor primitive-based control for leg exoskeletons during continuous multi-locomotion tasks," *Front. Neurobot.*, vol. 11, 2017, Art. no. 15.
- [23] A. d'Avella and E. Bizzi, "Shared and specific muscle synergies in natural motor behaviors," *Proc. Nat. Acad. Sci.* vol. 102, no. 8, pp. 3076–3081, 2005.
- [24] Y.-X. Liu and E. M. Gutierrez-Farewik, "Muscle synergies enable accurate joint moment prediction using few electromyography sensors," in *Proc. IEEE/RSJ Int. Conf. Intell. Robots Syst.*, 2021, pp. 5090–5097.
- [25] M. Ghislieri et al., "Muscle synergies extracted using principal activations: Improvement of robustness and interpretability," *IEEE Trans. Neural Syst. Rehabil. Eng.*, vol. 28, no. 2, pp. 453–460, Feb. 2020.
- [26] P. Kieliba et al., "How are muscle synergies affected by electromyography pre-processing ?," *IEEE Trans. Neural Syst. Rehabil. Eng.*, vol. 26, no. 4, pp. 882–893, Apr. 2018.
- [27] A. Saito et al., "Muscle synergies are consistent across level and uphill treadmill running," *Sci. Rep.*, vol. 8, no. 1, pp. 1–10, 2018.
- [28] H. J. Hermens et al., "European recommendations for surface electromyography, results of the SENIAM project," *Roessingh Res. Develop.*, Enschede, The Netherlands, 1999.
- [29] Vicon, "PyCGM2", Accessed: Sep. 2021. [Online]. Available: <https://pycgm2.github.io/pages/cgm23-overview.html>
- [30] M. J. Perry, *Gait Analysis: Normal and Pathological Function*. Thorofare, NJ, USA: SLACK, 2010.
- [31] F. Leboeuf et al., "P 120 - CGM2 : Proposal of an evolved conventional gait model," *Gait Posture*, vol. 65, pp. 436–437, 2018.
- [32] R. W. Schutz and M. E. Gessaroli, "The analysis of repeated measures designs involving multiple dependent variables," *Res. Quart. Exercise Sport*, vol. 58, no. 2, pp. 132–149, 1987.
- [33] A. d'Avella et al., "Combinations of muscle synergies in the construction of a natural motor behavior," *Nature Neurosci.*, vol. 6, no. 3, pp. 300–308, 2003.
- [34] H. Yokoyama et al., "Basic locomotor muscle synergies used in land walking are finely tuned during underwater walking," *Sci. Rep.*, vol. 11, no. 1, pp. 1–11, 2021.
- [35] S. Chvatal and L. Ting, "Common muscle synergies for balance and walking," *Front. Comput. Neurosci.*, vol. 7, 2013, Art. no. 48.
- [36] L. H. Ting and J. M. Macpherson, "A limited set of muscle synergies for force control during a postural task," *J. Neurophysiol.*, vol. 93, no. 1, pp. 609–613, 2005.
- [37] S. A. Chvatal et al., "Common muscle synergies for control of center of mass and force in nonstepping and stepping postural behaviors," *J. Neurophysiol.*, vol. 106, no. 2, pp. 999–1015, 2011.
- [38] E. Wentink et al., "Intention detection of gait initiation using EMG and kinematic data," *Gait Posture*, vol. 37, no. 2, pp. 223–228, 2013.
- [39] M. Townsend et al., "Variability and biomechanics of synergy patterns of some lower-limb muscles during ascending and descending stairs and level walking," *Med. Biol. Eng. Comput.*, vol. 16, no. 6, pp. 681–688, 1978.
- [40] A. Protopapadaki et al., "Hip, knee, ankle kinematics and kinetics during stair ascent and descent in healthy young individuals," *Clin. Biomech.*, vol. 22, no. 2, pp. 203–210, 2007.
- [41] D. Rimini et al., "Intra-subject consistency during locomotion: Similarity in shared and subject-specific muscle synergies," *Front. Hum. Neurosci.*, vol. 11, 2017, Art. no. 586.
- [42] D. Ao et al., "Evaluation of synergy extrapolation for predicting unmeasured muscle excitations from measured muscle synergies," *Front. Comput. Neurosci.*, vol. 14, 2020, Art. no. 108.